NUMERICAL SOLUTION OF INVISCID AND VISCOUS FLOWS USING WEIGHTED LEAST SQUARE SCHEME AND QUADRILATERAL OR TRIANGULAR MESH

JIŘÍ FÜRST[1]

Abstract. The article describes development of a high order finite volume method for solution of transonic flow problems. The method is based on a reconstruction procedure similar to weighted ENO. Our reconstruction procedure is based on least square method with data dependent weights which is much simpler to implement than ENO scheme. The computational results demonstrate the usability of this approach for solution of several flow problems in 2D and 3D using both structured and unstructured meshes.

Key words. FVM, method of lines, ENO, shock capturing, transonic flows.

AMS subject classifications. F 35Q30, 76H05, 65M12, 65M20, 65N99.

1. Introduction. This article deals with the numerical solution of Euler or Navier–Stokes equations describing motion of compressible inviscid or viscous gas

$$(1.1) \qquad \frac{\partial \rho}{\partial t} + \frac{\partial}{\partial x_j}\left(\rho u_j\right) = 0,$$

$$(1.2) \qquad \frac{\partial}{\partial t}\left(\rho u_i\right) + \frac{\partial}{\partial x_j}\left(\rho u_i u_j\right) + \frac{\partial p}{\partial x_i} = \frac{\partial \tau_{ij}}{\partial x_j},$$

$$(1.3) \qquad \frac{\partial E}{\partial t} + \frac{\partial}{\partial x_j}\left((E+p)u_j\right) = \frac{\partial}{\partial x_j}\left(u_i \tau_{ij}\right) - \frac{\partial q_j}{\partial x_j},$$

where ρ is density, u_i are components of velocity vector, p is pressure, E is total energy per volume unit, τ_{ij} is stress tensor, and q_j are components of heat flux (see e.g. [4]).

The solution can be obtained with standard finite volume method. However, the basic method of Godunov type often suffers from low accuracy. One possibility how to improve the accuracy of such method is the application of an interpolation procedure which tries to reconstruct pointwise values of the solution from their cell averages. The main problem of those interpolation procedures is their applicability for data with discontinuities and/or strong gradients. The so called ENO (i.e. *essentially non-oscillatory*) reconstruction has been developed (see e.g. [12], [14]) and transformed to finite volumes by many researchers at the end of last century. Nevertheless, the standard finite volume version of ENO or weighted ENO method (see [13], [7] etc.) is relatively complicated for general meshes. In fact, there is very few results obtained with ENO/WENO using unstructured meshes in 3D. On the other hand, the proposed WLSQR interpolation is simply extensible also for 3D (see last section of this article for an example).

[1]Department of Technical Mathematics, Faculty of Mechanical Engineering, Czech Technical University in Prague, Karlovo nám. 13, 120 00 Prague, Czech Republic.

We proposed in [10] a reconstruction procedure based on least square method combined with data dependent weights for avoiding interpolation across a discontinuity. Article [10] shows several applications of our weighted least square method namely for inviscid transonic flows in 2D channels and turbine cascades with piecewise linear reconstruction. Article [11] shows the extension to piecewise parabolic interpolation for scalar test case.

The aim of this article is to document some preliminary experiments concerning the choice of the weights in the reconstruction and to test the method for 3D inviscid flows and 2D viscous flows in complex geometries.

2. High order finite volume method. As a base for our numerical method we use standard finite volume method with data located in centers of polygonal cells. The basic low order semi-discrete method can be written as (see e.g. [4])

$$\frac{du_i(t)}{dt} = - \sum_{j \in \mathcal{N}_i} \mathcal{F}(u_i(t), u_j(t), \vec{S}_{ij}).$$
(2.1)

Here $u_i(t)$ is the averaged solution over a cell C_i, $\mathcal{N}_i$ denotes the set of indices of neighborhoods of C_i, $\vec{S}_{ij}$ is the scaled normal vector to the interface between C_i and C_j (oriented to C_j) and $\mathcal{F}$ denotes the so called numerical flux approximating physical flux through the interface between cells C_i and C_j. In our case we use the AUSM or AUSM+ flux [17], [16] nevertheless it is possible to use also another ones e.g. Roe's flux, Osher's flux etc.

A higher order method can be obtained by introducing a cell-wise interpolation $P(\vec{x}; u) = P_i(\vec{x}; u)$ for $x \in C_i$ into the basic formula. The higher order method is then formally

$$\frac{du_i(t)}{dt} = - \sum_{j \in \mathcal{N}_i} \mathcal{F}(P_i(\vec{x}_{ij}; u), P_j(\vec{x}_{ij}; u), \vec{S}_{ij}),$$
(2.2)

where $\vec{x}_{ij}$ is the center of interface between C_i and C_j.

The semi-discrete is then solved either by explicit Runge-Kutta method, either by implicit backward Euler method (see [8] or [11] for details).

3. Weighted least square interpolation. The most interesting part of the above mentioned method is the high order reconstruction (or interpolation). There are several reconstruction methods in the literature, but most of them are limited to structured meshes or to lower order of accuracy. We describe here only piecewise linear variant *weighted least square* (or shortly WLSQR) interpolation. Extension to piecewise parabolical case was given in [11].

We assume, that any reconstruction should satisfy following requirements:

1. **Conservativity**, i.e. the mean value of the interpolant $P(x; u)$ over any cell C_i should be equal to cell average of u, in other words

$$\int_{C_i} P(\vec{x}; u) \, d\vec{x} = |C_i| u_i.$$
(3.1)

2. **Accuracy**, i.e. for a given smooth function $\tilde{u}(\vec{x})$ with cell averages u_i the interpolant $P(\vec{x}; u)$ should approximate $\tilde{u}$:

$$P(\vec{x}; u) = \tilde{u}(\vec{x}) + \mathcal{O}(h^o),$$
(3.2)

where h is characteristical mesh size and o is the order of accuracy. This accuracy requirement is reformulated in the following way: let prolongate $P_i(\vec{x}; u)$ over cells in the vicinity of cell C_i. Then we request for such cells C_j

$$(3.3) \qquad \int_{C_j} P_i(\vec{x}; u)\, d\vec{x} = |C_j| u_j.$$

3. **Non-oscillatory**, i.e. the total variation of the interpolant should be bounded for $h \to 0$.

The interpolant $P_i(\vec{x}; u)$ is therefore obtained by minimizing error in (3.2) for C_j being the neighborhoods of C_i with respect to (3.1). In order to mimic weighted ENO method we introduce data dependent weights:

$$(3.4) \qquad P_i(\vec{x}; u) = \arg\min \sum_{j \in \mathcal{N}_i} \left[w_{ij} \left(\int_{C_j} \tilde{P}(\vec{x}; u)\, d\vec{x} - |C_j| u_j \right) \right]^2,$$

where minimum is take over over all linear polynomials $\tilde{P}$ satisfying (3.1), in other words, we define P_i as a polynomial satisfying (3.1) and minimizing errors in (3.3) in L_2 norm. Weights w_{ij} should depend on u and they should be high when u is smooth and small when there is a discontinuity in u. This behavior is similar to ENO reconstruction which can be for piecewise linear polynomials in 1D written as WLSQR reconstruction with weights being either 1 or 0. In our case, we chose

$$(3.5) \qquad w_{ij} = \sqrt{\frac{h^{-r}}{\left| \frac{u_i - u_j}{h} \right|^p + h^q}},$$

with p, q, and r being constants (e.g. $p = 4$, $q = -3$, $r = 3$).

4. Choice of parameters of weights in WLSQR interpolation. The coefficient r is for scaling, which can be useful for high aspect ratio cells. Its role is not analyzed here and it was chosen to be $r = 3$. The ratio p/q determines the behavior of the weight: the weight is $\mathcal{O}(h^{-r-q})$ when $|\Delta_{ij}u/h| << h^{q/p}$ (here $\Delta_{ij}u = u_i - u_j$), and $\mathcal{O}(h^{-r}|\Delta_{ij}u/h|^{-p})$ when $|\Delta_{ij}u/h| >> h^{q/p}$.

Let assume smooth function u. Then $\Delta u_{ij}/h$ is bounded independently of h and the weight should be relatively large in that case. It happens for example for $p > 0$ and $q \le 0$ (the weight is at least $\mathcal{O}(h^{-r/2})$).

On the other hand, when there is a discontinuity in u, then $\Delta_{ij}u/h = \mathcal{O}(h^{-1})$ and the weight should be relatively small. In fact, it is at most $\mathcal{O}(h^{(p-r)/2})$ assuming $p > 0$.

4.1. Theoretical analysis for simplified cases. The complete analysis of accuracy and stability (in the sense of total variation of the interpolation) is very complicated for general multidimensional case. We give here a preliminary results obtained for equidistant meshes in 1D and piecewise linear interpolant.

Denote the mesh spacing by h, then the interpolant is defined by

$$(4.1) \qquad P_i(x) = \zeta_i + \sigma_i x, \text{ for } x \in (x_{i-1/2}, x_{i+1/2}).$$

The conservativity requirement yields $\zeta_i = u_i$. Assuming the accuracy requirements for two neighborhoods and weights w one obtains the following system of equations

for single unknown σ_i

$$(4.2) \qquad w_{i+1/2}u_{i+1} = w_{i+1/2}\left(u_i + h\sigma_i\right),$$

$$(4.3) \qquad w_{i-1/2}u_{i-1} = w_{i-1/2}\left(u_i - h\sigma_i\right).$$

The system is overdetermined and we solve it in the least square sense, i.e. we minimize the functional at the right hand side of (3.4). The solution to this system gives

$$(4.4) \qquad \sigma_i = \frac{w_{i+1/2}^2(u_{i+1} - u_i) + w_{i-1/2}^2(u_i - u_{i-1})}{h(w_{i+1/2}^2 + w_{i-1/2}^2)}.$$

Assuming smooth function $u(x)$ and applying Taylor expansions to u one gets

$$(4.5) \qquad \sigma_i = u_x(x_i) + \frac{h}{2}u_{xx}(x_i)\frac{w_{i+1/2}^2 - w_{i-1/2}^2}{w_{i+1/2}^2 + w_{i-1/2}^2} + \mathcal{O}(h^2).$$

Next, since $\Delta_{ij}u/h$ is bounded independently on h, the weights are bounded (for sufficiently small h and $q \leq 0$) by $\frac{1}{2}h^{-r-q} \leq w_{ij}^2 \leq h^{-r-q}$. Therefore the term by $h/2u_{xx}$ is bounded by 2 from above.

The following lemma follows directly from the last formulas:

LEMMA 4.1. *Assume a sufficiently smooth function $u(x)$ having cell averages u_i and weights $w \neq 0$. Then the piecewise linear WLSQR interpolation polynomial with $p > 0$ and $q \leq 0$ approximates $u(x)$ with second order of accuracy, i.e.*

$$(4.6) \qquad P(x;u) = u(x) + \mathcal{O}(h^2).$$

Another issue is the stability for non-smooth data. It can be examined in the terms of total variation. Up to now we do not have general results concerning discontinuous case, therefore we mention here only special case with data corresponding to a shock given by $u(x) = 1$ for $x < x_{shock}$ and $u(x) = 0$ for $x \geq x_{shock}$. Without loss of generality we assume, that the shock is located inside cell with index 0. It means, that the cell averaged values u_i will be $u_i = 1$ for negative i, $u_i = 1$ for positive i and $u_0 = c$ where $c \in [0,1]$ corresponds to exact location of the shock inside cell. With this data we can compute weights

$$(4.7) \qquad w_{-1/2}^2 = h^{p-r}/\left((1-c)^p + h^{p+q}\right),$$

$$(4.8) \qquad w_{1/2}^2 = h^{p-r}/\left((c^p + h^{p+q}\right),$$

$$(4.9) \qquad w_{3/2}^2 = h^{p-r}/h^{p+q}.$$

The formula (4.4) yields

$$(4.10) \qquad \sigma_0 = -\frac{1}{h}\frac{(c^p + h^{p+q})(1-c) + [(1-c)^p + h^{p+q}]c}{c^p + (1-c)^p + 2h^{p+q}},$$

$$(4.11) \qquad \sigma_1 = -\frac{1}{h}\frac{h^{p+q}c}{2h^{p+q} + c^p}.$$

At first we will compute magnitude of overshoot for interface between cells 1 and 2 denoted by $\delta_{3/2}$.

$$(4.12) \qquad \delta_{3/2} = |h/2\sigma_1| = \frac{h^{p+q}c}{4h^{p+q} + 2c^p}.$$

The value of c can be arbitrary in $[0, 1]$ (and may depend on h), so we analyse two cases (assuming always $p > 1$):
- assume $c^p < h^{p+q}$, then

$$(4.13) \qquad \delta_{3/2} \leq \frac{h^{p+q}c}{4h^{p+q}} \leq 0.25h^{1+q/p},$$

- assume $c^p \geq h^{p+q}$ in this case

$$(4.14) \qquad \delta_{3/2} \leq \frac{h^{p+q}c}{2c^p} \leq 0.5h^{1+q/p+p+q}.$$

In both cases we have for small h (assuming $p + q \leq 0$)

$$(4.15) \qquad \delta_{3/2} \leq h^{1+q/p}.$$

The overshoot at the interface $-1/2$ can be estimated in the same way.

The calculation of magnitude of overshoot $\delta_{1/2}$ is much more complicated. Numerical experiments with $p = 4$, $q \in [-10, 10]$, $c \in [0, 1]$, and $h > 0$ shows, that the overshoot $\delta_{1/2} = -\min(0, u^L_{1/2}, u^R_{1/2})$ has maximum for $c = 0$. Here $u^L_{1/2}$ and $u^R_{1/2}$ are the values of the interpolant at the left and right side of interface $1/2$. Assuming validity of this hypothesis we have the following estimate for $\delta_{1/2}$ (for small h):

$$(4.16) \qquad \delta_{1/2} \leq \frac{h^{p+q}}{2 + 4h^{p+q}} \leq \frac{h^{p+q}}{2}.$$

Moreover, it is easy to prove that the overshoot can occur only for $c < 1/2$. It means, that $\delta_{-1/2}$ or $\delta_{1/2}$ is equal to zero.

Summing all those things together we can conclude, that (at least) for $p = 4$ and $q \in [-10, 10]$ the total variation of interpolant is for the case of a shock

$$(4.17) \quad TV(P(x; u)) \leq 1 + 2 \left(\delta_{-1/2} + \delta_{1/2} + \delta_{1/2} \right) \leq TV(u) + 4h^{1+q/p} + h^{p+q}.$$

This yields the following lemma:

LEMMA 4.2. *Assume weights with*[1]

$$(4.18) \qquad p + q \geq 0, \ and \ p > 0.$$

Then the total variation of the interpolant of data given by a single shock with constant states at both sides will be bounded independently of h as $h \to 0$.

Note that this simplified analysis does not give any condition on r. Moreover, it is not clear if the conditions given in the lemma 4.2 would apply also for more complicated configurations or for multidimensional systems.

4.2. Numerical experiments. In the previous section we have discussed some theoretical aspects of the choice of p, q, and r in the definition of weight. We obtained some necessary conditions for simple scalar one-dimensional cases. However, it is not clear whether those conditions apply also for multidimensional systems of equations. Therefore we present results of several calculation with different values of p, q, r and we compare their quality.

First case is the transonic flow through a test channel (the so called GAMM channel, see fig. 4.1). The solution was obtained using the implicit version of our

---

[1]From $p > 0$ and $p + q \geq 0$ follows $1 + q/p \geq 0$ and therefore $\delta_{3/2} \to 0$ in (4.15).

method using a mesh with 90×30 quadrilateral cells. Figure 4.2 shows calculated distribution of Mach number and convergence history for different values of p, q, r. Since the calls have aspect ratio close to one, the value of r should not be to important for this case. Therefore we set $r = 3$ and we changed only the ratio of p and q. One can see, that the convergence history is similar for all cases starting from $p = 4$, $q = 0$ to $p = 4$, $q = -4$. The distribution of Mach number however differs from case to case. By comparison with results obtained with other methods (see e.g. [3], [9] etc.) we can see, that the triplet $p, q, r = 4, 0, 3$ does not resolve well the structure of the shock. On the other hand, triplets $4, -2, 3$ and $4, -3, 3$ do very good job. There are no significant overshoots and the Zierep's singularity can be identified behind the shock.

(a) Geometry of the channel

(b) Mesh with 90×30 cells

FIG. 4.1. *2D GAMM channel*

(a) Distribution of Mach number with detail of the shock wave
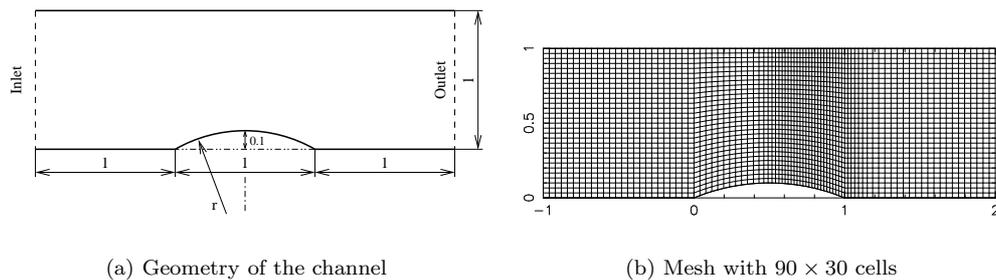
(b) Convergence history
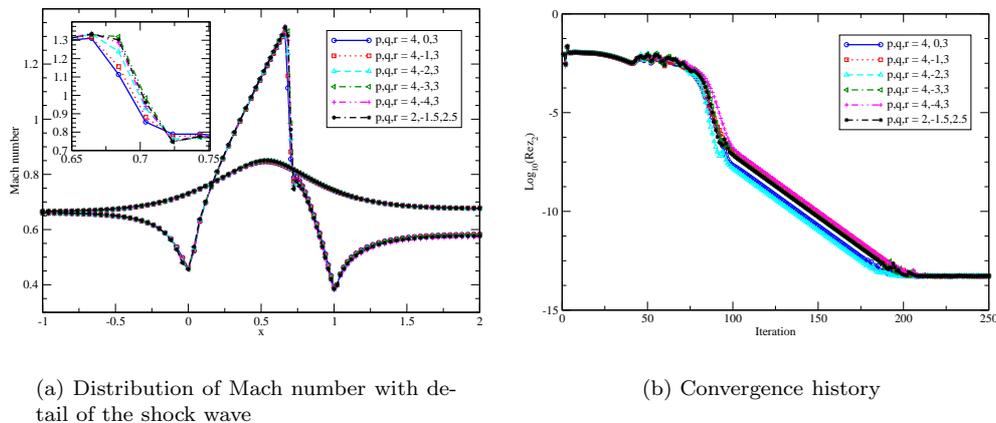
FIG. 4.2. *Distribution of Mach number along walls and convergence history for 2D GAMM channel test case.*

Another case is the transonic flow over NACA 0012 profile with inlet Mach number $M_\infty = 0.8$ and inlet angle $\alpha_1 = 1.25°$. The computation was made using a structured mesh with 168×40 quadrilateral cells which was used for this test case. It can be seen at the fig. 4.3 that triplets $p, q, r = 4, -1, 3$, $4, -2, 3$, and $4, -3, 3$ resolve shock wave with tiny overshoots (almost invisible for $4, -1, 3$, higher for lower values of q). Convergence to steady state was very good for $4, -2, 3$ and $4, -3, 3$ whereas it stalls for $4, -1, 3$ and it diverges for $4, -4, 3$.

Figure 4.4 shows isolines of Mach number obtained with obtained with $p, q, r = 4, -2, 3$ and comparison of computed distribution of pressure coefficient c_p with results found in [1] and [6]. One can see, that there are big differences in the position of the shock wave. Nevertheless, the WLSQR method shows at least qualitatively good agreement with other results with exception of those of Zanetti.
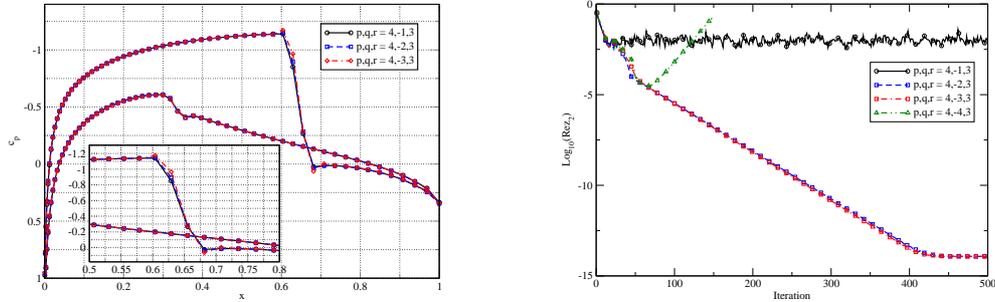
FIG. 4.3. *Distribution of c_p for different weights (left) and convergence history (right) for flow around NACA 0012 profile at $M_\infty = 0.8$ and $\alpha_1 = 1.25°$.*
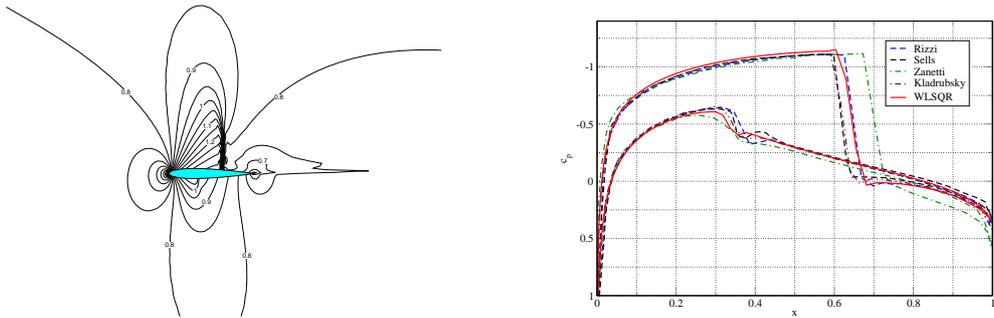
FIG. 4.4. *Isolines of Mach number (left) and comparison of c_p obtained using $p, q, r = 4, -2, 3$ with results found in references [1] and [6] (right) for flow around NACA 0012 profile at $M_\infty = 0.8$ and $\alpha_1 = 1.25°$.*

Those numerical experiments off course did not give complete answer on the question of the choice of weights in WLSQR methods. However, they says, that the weights with p, q, r being $4, -2, 3$ or $4, -3, 3$ are at least in some cases suitable for applications in calculations of transonic flows.

5. Application to several flow problems. In the last section we show several flow problems which were solved with the help of WLSQR interpolation incorporated into a basic finite volume scheme.

5.1. 2D inviscid flow through turbine cascade. As an example of the application of our method is the inviscid flow through a 2D turbine cascade with inlet Mach number $M_1 \approx 0.3$, inlet angle $\alpha_1 = 19.3°$ and outlet Mach number $M_2 = 1.2$. The figure 5.1 shows the results obtained using an unstructured mesh with triangular cells. The mesh is adaptively refined in order to resolve better shock waves. Figure 5.2 shows the interferogram of the flow field obtained at the Institute of Thermomechanics [18] and the comparison of measured distribution of pressure with our

numerical results using three meshes. One can see relatively good agreement both in the structure of the flow field and in the distribution of pressure. There are still some differences in the pressure distribution at $x \approx 0.8$. This difference may be caused by neglected viscosity.
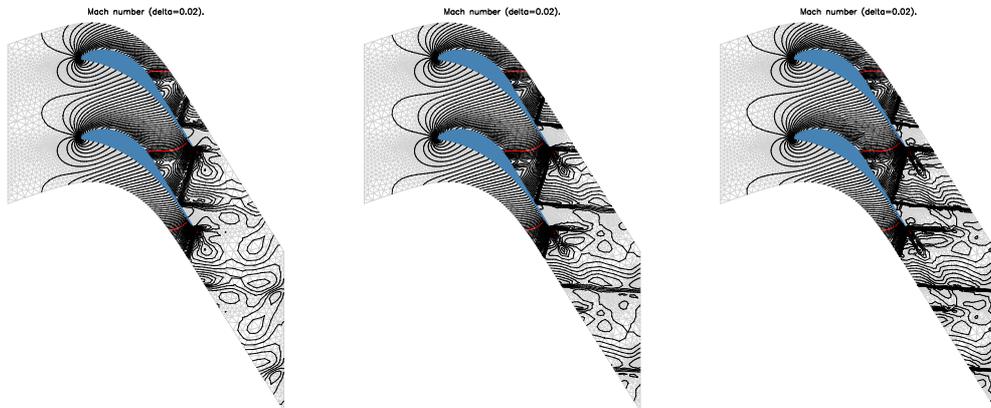
FIG. 5.1. *Isolines of Mach number for inviscid transonic flow through 2D turbine cascade with adaptive mesh refinement (5646 triangles, 7952 triangles, 11440 triangles)*
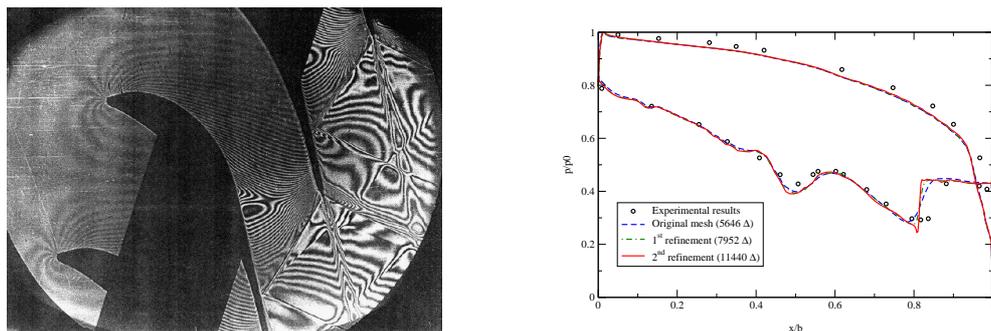
FIG. 5.2. *Comparison of numerical results with experimental data for transonic flow through a 2D turbine cascade; interferogram and distribution of pressure.*

5.2. 2D viscous flow over a profile. Another case is the application of the method for viscous transonic flows in turbulent regime at high Reynolds number. The flow is described by the so called Reynolds averaged Navier–Stokes equation and the turbulence is modeled by the TNT $k-\omega$ model of Kok [15]. The domain is discretized using a structured hyperbolic mesh with 164×96 quadrilateral cells with refinement in the direction normal to the profile prepared by A. Jirásek. Normal size of first cell is approximately $\Delta y_1 = 10^{-5}$ and the size grows exponentialy with $\Delta y_{j+1}/\Delta y_j \leq 1.1$. Inlet and outlet conditions correspond to the flow with $M_\infty = 0.734$, $\alpha_1 = 2.54°$, and $Re = 6.5 \cdot 10^6$ which corresponds to CASE-9 from [2] with tunnel corrections Figure 5.3 shows isolines of Mach number, isolines of turbulent Reynolds number defined as a ratio of turbulent viscosity μ_T and laminar viscosity μ_L, and a comparison of computed pressure coefficient and skin friction with experimental data [2].
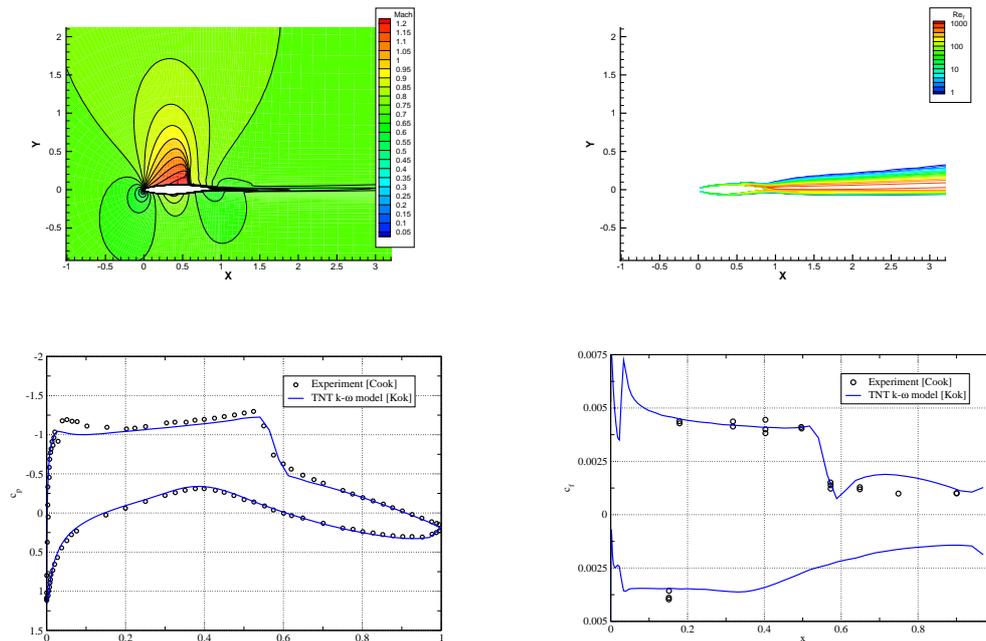
FIG. 5.3. *Solution of turbulent viscous flow over RAE2822 profile, $M_\infty = 0.734$, $\alpha_1 = 2.54°$, $Re = 6.5 \cdot 10^6$, isolines of Mach number (top left), turbulent Reynolds number (top right), ditribution of pressure coefficient (bootom left), and skin friction coeeficient (bottom right).*

5.3. 3D inviscid flow through a turbine cascade. Last example is the inviscid transonic flow through 3D turbine cascade. We assume that the flow is periodic from blade to blade and therefore it is possible to solve the flow field just in one period. The domain is discretized using a structured mesh with hexahedral cells. The inflow and outflow conditions depend on the radius. Figure 5.4 compares the distribution of Mach number obtained with the WLSQR method with AUSM flux using a structured mesh with $100 \times 20 \times 20$ cell. It can be seen, that the solution is comparable to the reference solution obtained with TVD MacCormack scheme [8] with finer mesh having $200 \times 40 \times 40$ cells. Similar results were also obtained by J. Halama [5] using cell vertex Ni's scheme with Jameson's artificial viscosity.

6. Conclusion. The analysis of the WLSQR method given in this article shows some preliminary results concerning the stability of the interpolation procedure for discontinuous data. The analysis was done only in very simple cases. However, numerical experiments show relatively good properties of the method for wide range of transonic flow calculation. The distribution of c_p for NACA 0012 shows, that the method produces small overshoots near the shock wave. In many applications, such overshoots do not matter (provided that they do not blow up). However, the choice of the weight should be more examined especially for the case of high aspect ratio cells.
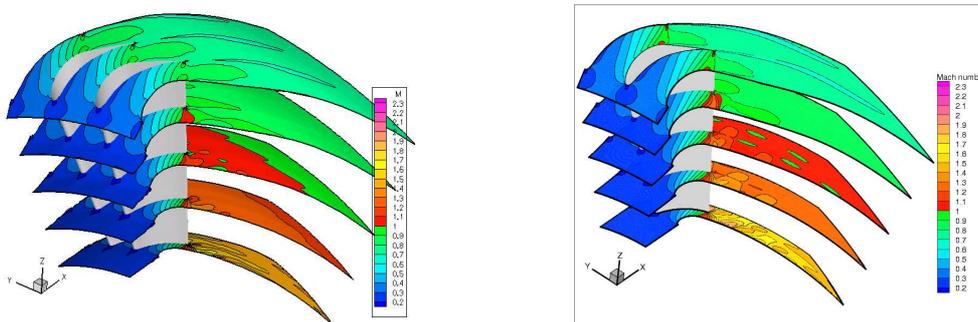
FIG. 5.4. *Isolines of Mach number for inviscid flow through a 3D turbine stator, WLSQR method on the left (coarser mesh), TVD MC scheme on the right (finer mesh).*

REFERENCES

[1] H. VIVIAND A. RIZZI, EDITOR. *Numerical Methods for the Computation of Inviscid and Viscous Transonic Flows with Shock Waves.* Vieweg, 1981.

[2] P. H. COOK, M. A. McDONALD AND M. C. P. FIRMIN. Aerofoil 2822 - pressure distributions, boundary layer and wake measurements. Technical Report AR 138, AGARD, 1979.

[3] V. DOLEJŠÍ. *Adaptive Higher Order Methods for Compressible Flows.* PhD thesis, Charles University, Faculty of Mathematics and Physics, 2003.

[4] M. FEISTAUER, J. FELCMAN, AND I. STRAŠKRABA. *Mathematical and Computational Methods for Compressible Flow.* Numerical Mathematics and Scientific Computation. Oxford University Press, 2003.

[5] J. FOŘT, J. FÜRST, J. HALAMA AND K. KOZEL. Numerical simulation of 3D transonic flow through cascades. *Mathematica Bohemica*, 126(2):353–361, 2001.

[6] J. FOŘT, A. JIRÁSEK, M. KLADRUBSKÝ AND K. KOZEL. Numerické řešení nevazkého transsonického proudění kolem profilu. *Letecký zpravodaj*, (1):2–6, 1998.

[7] O. FRIEDRICH. Weighted essentially non-scillatory schemes for the interpolation of mean values on unstructured grids. *Journal of Computational Physics*, 144(1):194–212, 1998.

[8] J. FÜRST. *Numerical modeling of the transonic flows using TVD and ENO schemes.* PhD thesis, ČVUT v Praze and l'Université de la Méditerranée, Marseille, February 2001.

[9] J. FÜRST, M. JANDA, AND K. KOZEL. Finite volume solution of 2D and 3D Euler and Navier-Stokes equations. In P. Penel, J. Neustupa, editor, *Mathematical Fluid Mechanics*, pages 173–193. Birkhäuser Verlag, 2001.

[10] J. FÜRST AND K. KOZEL. Numerical solution of transonic flows through 2D and 3D turbine cascades. *Computing and Visualization in Science*, 4(3):183–189, February 2002.

[11] J. FÜRST AND K. KOZEL. Second and third order weighted ENO scheme on unstructured meshes. In F. Benkhaldoun and R. Vilsmeier, editors, *Finite Volumes for Complex Applications. Problems and Perspectives.* Hermes, July 2002.

[12] A. HARTEN, B. ENQUIST, S. OSHER AND S. CHAKRAVARTHY. Uniformly high order essentially non-oscillatory schemes III. *Journal of Computational Physics*, 71:231–303, 1987.

[13] A. HARTEN AND S. R. CHAKRAVARTHY. Multi-dimensional ENO schemes for general geometries. Technical Report 91-76, ICASE, September 1991.

[14] G.-S. JIANG AND C.-W. SHU. Efficient implementation of weighted ENO schemes. *Journal of Computational Physics*, 126:202–228, 1996.

[15] J. C. KOK. Resolving the dependence onfree stream values for the k-omega turbulence model. Technical Report NLR-TP-99295, NLR, 1999.

[16] M. S. LIOU. A sequel to AUSM: AUSM+. *Journal of Computational Physics*, (129):364–82, 1996.

[17] Y. WADA AND M.-S. LIOU. A flux splitting scheme with high-resolution and robustness for discontinuities. *AIAA Paper*, 1994.

[18] P. Šafařík. Experimental data from optical measurement tests on a transonic turbine blade cascade. In *Measuring Techniques for Transonic and Supersonic Flow in Cascades and Turbomachines*, number 20, pages 0–14. ETH Zurich, 1997.